Modern Physics Letters B
Vol. 28, No. 26 (2014) 1450208 (12 pages)

DOI: 10.1142/S021798491450208X

World Scientific
www.worldscientific.com

Study the structure and performance of thermal/plasma modified Au nanoparticle-doped TiO_2 photocatalyst

Asif Mahmood[*,**], Shahid M. Ramay[†], Yousef S. Al-Zaghayer[*,‡], Shahid Atiq[§], Iftikhar Ahmad[¶], Muhammad Ali Shar[¶] and Salah Din Khan[‖]

[*] *Department of Chemical Engineering, College of Engineering, King Saud University, Riyadh, Saudi Arabia*
[†] *Department of Physics and Astronomy, College of Science, King Saud University, Riyadh, Saudi Arabia*
[‡] *Industrial Catalysts Research Chair, King Saud University, Riyadh, Saudi Arabia*
[§] *Center of Excellence in Solid State Physics, University of the Punjab, New Campus, Lahore, Pakistan*
[¶] *Center of Excellence for Research in Engineering Materials, Mechanical Engineering Department, College of Engineering, King Saud University, Riyadh, Saudi Arabia*
[‖] *Sustainable Energy Technologies Center, King Saud University, Riyadh, Saudi Arabia*
[**] *ahayat@ksu.edu.sa*

Received 9 August 2014
Revised 14 September 2014
Accepted 16 September 2014
Published 8 October 2014

This study describes the influence of thermal/plasma treatments on the structure and photocatalytic performance of the Au-doped TiO_2 catalyst. Au (gold) nanoparticles were attached on TiO_2 (Titania) nanoparticle surfaces by conventional deposition precipitation technique and the resulting catalysts were subsequently modified with thermal (at 450°C under vacuum) and plasma (at an ambient temperature under Argon atmosphere for 20 min) treatments. Structural characterization of the modified catalysts was performed by diverse analytical techniques and the photocatalytic activity was evaluated by assessing the degradation of the methylene blue (MB) in water under UV (ultra-violet) irradiations. Results showed that the thermal/plasma treatment significantly influenced the structural features of Au-doped TiO_2 catalyst by altering the morphology, increasing the Au nanoparticles population, improving the Au/TiO_2 catalytic activity, changing the textural properties and reducing the band gap energies thus tuned Au-doped TiO_2 catalyst to higher efficiency. Thermal/plasma treated Au-doped TiO_2 was found to exhibit higher photocatalytic activity than the as-synthesized (pristine sample). This improvement in photocatalytic activity might be due to the cathodic influence of gold in suppressing the electron–hole recombination during the reaction.

Keywords: Photocatalysts; Au/TiO_2; thermal; plasma; methylene blue.

[**]Corresponding author.

1. Introduction

Photocatalytic oxidation techniques have created a center of attention to their prospective practical applications in various fields especially for water disinfection. Foreseeing the potential applications in advanced technologies like solar cells, water decontamination, air purification and hydrogen production, rigorous research is needed to develop novel and most effective photocatalysts materials than those available today.[1–6] TiO_2 is one of the most potential photocatalysts used for the degradation of organic pollutants and also owes added benefits such as physical and chemical stability, intoxicate, relatively economical, anticorrosive characteristics, environmentally friendly, and outstanding photocatalytic performance in comparison with contemporary competitor semiconductor materials. Therefore, TiO_2 has got a great deal of research interests among the commercially employed photocatalysts over the last three decades.

Monometallic catalysts alone and in combination with the oxide catalysts have demonstrated great potential for increasing the catalytic activity.[7–9] In this regard, several research groups attempted noble metals (Au, Pt, Pd, CuS) doped TiO_2 catalysts proclaimed Au, the most attractive metal by confirming its compatibility with TiO_2.[10] Indeed, Fermi level (E_f) of TiO_2 is slightly higher than the Au nanoparticles and this feature allows the photo-excited electrons to efficiently transfer from the TiO_2 surface to Au nanoparticles.[11] However, synthesis parameters such as contact time, pH values, temperature conditions and the catalyst activation procedures are imperative to establish interfacial contact between Au nanoparticles and TiO_2.[12–15] Based on the Au absorption band that exists between 500–600 nm, it has been suggested that the Au-doped TiO_2 catalyst has also capability to enhance the photo response of the TiO_2 under visible-light region.[11] In this context, numerous research groups proposed that the stimulation of electrons at the surface plasmon of the Au may probably be helpful in order to relocate the electron to the low energy conduction band (CB) of the TiO_2, which is photocatalytically immobile with visible-light.[16–18] Furthermore, a photocatalytic process depends on the generation of electron–hole pairs by means of band gap radiation that can give rise to redox reactions with the species adsorbed on the surface of the photocatalysts.[19]

Despite the catalytic behaviors of Au-doped TiO_2 catalysts, which have already been extensively studied however the use of Au for improving photocatalysis in wastewater treatment need further attention.[12–15] In this context, obtaining higher photocatalytic activity in Au-doped TiO_2 catalyst by Au nanoparticles morphology and dimensions manipulation is thus interesting. Herein we report the modification of the exiting Au-doped TiO_2 catalyst with thermal/plasma processes and the influence of these processes on the structure and photocatalytic activity of the modified Au-doped TiO_2 catalyst is presented in this study.

2. Experimental Method

2.1. *Materials*

Gold (III) chloride trihydrate ($HAuCl_4 \cdot 3H_2O$, $\geq 99.9\%$ pure, Sigma-Aldrich), titanium dioxide (TiO_2, Degussa P25, surface area 45 $m^2\ g^{-1}$, $> 99.5\%$ pure), sodium hydroxide (NaOH, $\geq 98\%$ pure, Sigma-Aldrich), deionized water (H_2O, Sigma-Aldrich), and methylene blue (MB) ($C_{16}H_{16}ClN_3S_4 \cdot xH_2O$, Qualikems Fine Chem. Pvt. Ltd) were used as such without further purification.

2.2. *Synthesis techniques*

Au-doped TiO_2 photocatalyst was prepared by deposition precipitation (DP) process using Gold (III) chloride trihydrate ($HAuCl_4 \cdot 3H_2O$) as Au precursor and nonporous Degussa P25 as TiO_2 support. With the assistance of NaOH solution, the Au precursor solution was neutralized slowly under vigorous stirring conditions to pH 7 at 70°C and then mixed with a TiO_2 suspension by keeping the solution temperature at 35°C. The pH value of the resulting synthesized mixture was maintained at 70°C for 2 h. The mixture was then filtered and the residue powder was then washed repeatedly with deionized water and then the residue was finally dried at 80°C for 12 h, using vacuum oven. Some portion of the synthesized Au-doped TiO_2 catalyst was thermally treated at 450°C under 0.05 mTorr for 4 h. Finally, both (as prepared and thermally treated) catalysts were separately plasma sputtered at room temperature in 26 mTorr Ar for 30 min.

2.3. *Catalysts characterization*

Structural characterizations of all the Au-doped TiO_2 photocatalysts were performed by using X-ray diffractometer (XRD) (Brucker, D8 diffractometer) using Cu-Kα radiations ($\lambda = 1.5406$ Å) from 20° to 70° in 0.05° increments. The morphology of the as-synthesized (Pristine sample) and modified (thermal/plasma treated) photocatalysts were examined by scanning electron microscopy (SEM), JEOL JSM-7600F, FESM, Japan and elemental analysis was carried out by attached EDS analysis (Oxford instruments, UK). Transmission electron microscopy (TEM) studies were done by using JEOL 2100F, FEG–TEM, Japan. The specific surface area, pore volume and average pore diameter of the catalysts were measured using Micromeritics Tristar ASAP 2020 surface area and porosity analyzer by N_2 adsorption data at 77 K according to the standard Brunauer Emmett Teller (BET) procedure. For each analysis 0.25 g of catalyst was used. Prior to analysis, the degassing of the samples was done at 200°C for 2 h to remove the moistness and weakly adsorbed gases from the catalyst surface. The absorbance spectra were recorded on a UV-Vis spectrophotometer (Labomed-2950, USA). UV-Vis diffuse reflectance spectroscopy measurements were carried out to calculate the energy band gaps (E_g) of the synthesized composites using PerkinElmer's LAMBDA 35 UV-Vis systems with integrating sphere accessory.

2.4. *Photocatalytic activity measurements*

In this study, MB was exploited as pollutant molecule. The photocatalytic degradation of MB was carried out in a rectangular quartz reactor ($30 \times 40 \times 60$ mm^3). An MB aqueous solution (1.16×10^{-5} M) was photocatalyzed in a quartz reactor at room temperature (25°C) under the UV light irradiation. In order to maintain the temperature of MB solution in the photo-reactor, cold water was circulated around the solution. A high-pressure mercury lamp (450 W, principal wavelength 365 nm and luminous intensity 0.4 mWcm^{-2}) served as the UV light source. 100 mg catalyst powders were dispersed into 100 ml MB aqueous solution (10 mg/L). Prior to irradiation, the suspension was sonicated in the dark to disperse the catalyst in dye solution and particular attention was given to the continuous stirring of the solution during the whole experiment. After irradiation at a given reaction time (0 min to 495 min by an increment of 45 min), about 2 mL of the mixed suspensions were extracted and filtered to separate the catalyst from the dye solution then the absorbance and degradation rates were determined by a UV-Vis spectrophotometer. The scanning wavelength range was from 300 nm to 750 nm.

3. Results and Discussion

3.1. *Structural analysis*

Figure 1 shows the XRD patterns of all catalyst samples and the peaks positions are well agreed with the reflection of TiO_2 anatase crystal structure (JCPS card no. 00-001-0562). However, no peaks from any other impurities were observed, which indicate the high purity of the obtained pure and Au-doped TiO_2. The peaks

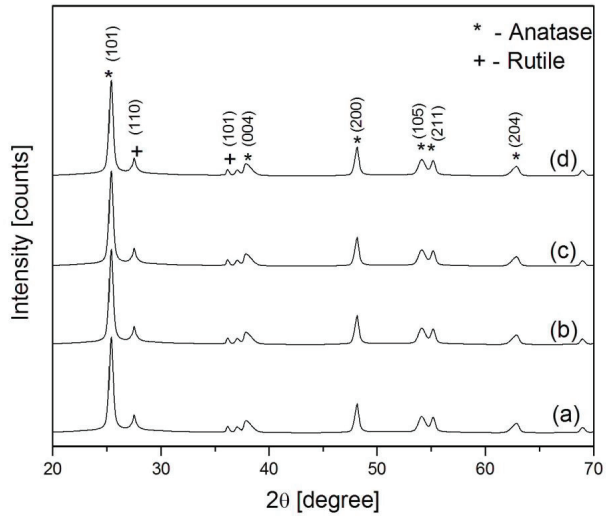

Fig. 1. XRD patterns of Au/TiO_2 catalysts: (a) pristine, (b) thermal, (c) plasma and (d) thermal/plasma treated.

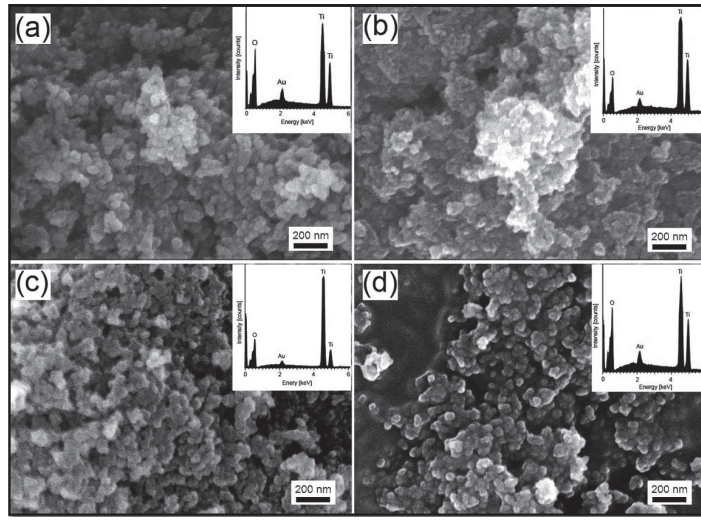

Fig. 2. SEM micrographs of the Au/TiO_2 catalysts: (a) pristine, (b) thermal, (c) plasma and (d) thermal/plasma treated.

corresponding to oxides of Au were not observed even for 1 wt.% substituted samples. Au peaks could not be identified in Fig. 1 and this may be due to the (i) high crystalline features of TiO_2 phase, which possibly shed the Au peaks and (ii) relative low concentration of Au nanoparticles in catalyst. Even after thermal/plasma treatment, no extra peaks were observed. Literature indicates that the TiO_2 rutile phase starts appearing at around 450°C in sol–gel materials, however, this suggests the presence of TiO_2 anatase, as major phase in our samples. Furthermore, presence of Au suppresses the TiO_2 crystalline phase conversion from anatase to the rutile, as reported earlier.[20,21]

Particle morphology of pristine sample is evident from the SEM image shown in Fig. 2(a). However; coalesce of catalyst nanoparticles shown in Fig. 2(b) occurred after thermal treatment at 450°C. Plasma treated samples exhibited rough and porous features [Fig. 2(c)], whereas these porous features were expanded in thermal/plasma treated samples as shown in Fig. 2(d).

Based on these porous structures, it may be postulated that the thermal/plasma treated samples might have enhanced photocatalytic activity owning high porosity. Furthermore, characteristic peaks recorded in the EDX spectra elucidate the presence of Au [Au in Fig. 2(a) $\sim$0.76 wt.%, in Fig. 2(b) $\sim$0.77 wt.%, in Fig. 2(c) $\sim$0.84 wt.% and in Fig. 2(d) $\sim$0.85] and other elemental constituents of the catalysts such as Ti, O as shown in insets of Figs. 2(a)–2(d). TiO_2 shows an intense peak around 4.44 keV. There are some Au peaks around 2.2 keV in the EDX pattern and this observation gave convincing evidence for the presence of Au on the surface of TiO_2.

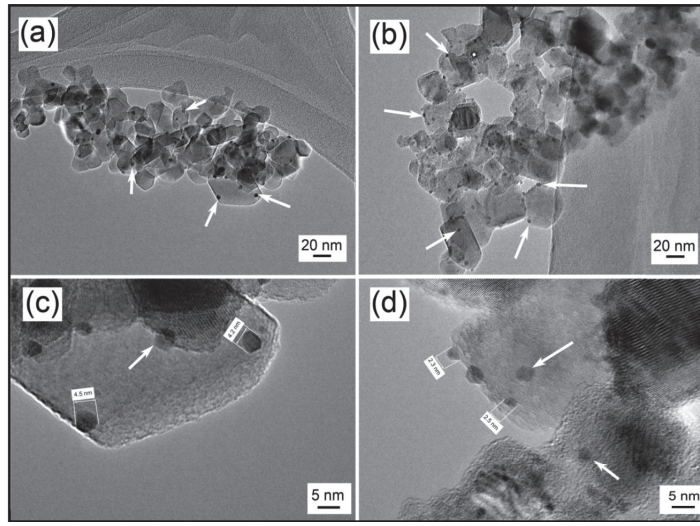

Fig. 3. TEM images of Au-doped TiO_2 catalysts samples: (a) pristine-indicating the attachment of Au nanoparticles (white arrows) on TiO_2 support, (b) thermal/plasma treated samples exhibiting fine Au nanoparticles at TiO_2 surfaces and Au nanoparticles at higher magnification, (c) prestine samples and (d) thermal/plasma treated samples showing very fine Au nanoparticle size.

TEM studies are very helpful in understanding the exact morphology, structure, dimensions, and distribution of Au nanoparticles on the base TiO_2 support as shown in Fig. 3. Although the same amount of Au nanoparticles were deposited during the catalysts preparation, but thermal modification followed by plasma treatment substantially affected the size and population of the Au nanoparticles on the surfaces of TiO_2 support than untreated samples as displayed in Fig. 3(b).

Quantitative analysis further confirmed the size refinement of the Au nanoparticles for modified catalyst (2–3 nm), shown in Fig. 3(d), compared to untreated samples which showed diameters in the range of 4–5 nm [Fig. 3(c)]. The reduction in the diameters of Au nanoparticles may be attributed with the plasma sputter processing, (i) it is quite possible that the Au nanoparticles undergone sever mechanical loading upon plasma ions bombing resulting in the compaction of Au nanoparticles into smaller size and (ii) the other possibility is the disintegration of the Au nanoparticles under severe plasma sputtering conditions which probably turned nanoparticles to smaller dimensions.[22] Furthermore, high resolution HR-TEM studies further confirm the size confinement of the Au nanoparticles after thermal/plasma treatment, as exhibited in lattice resolved images of the Au-doped TiO_2 catalyst (see Fig. 4).

HR-TEM images recorded on individual Au-doped TiO_2 catalyst constituent provide further insight into the structure and the catalyst constituents. Lattice resolved TEM images, Fig. 4, clearly shows very small Au nanoparticles composed

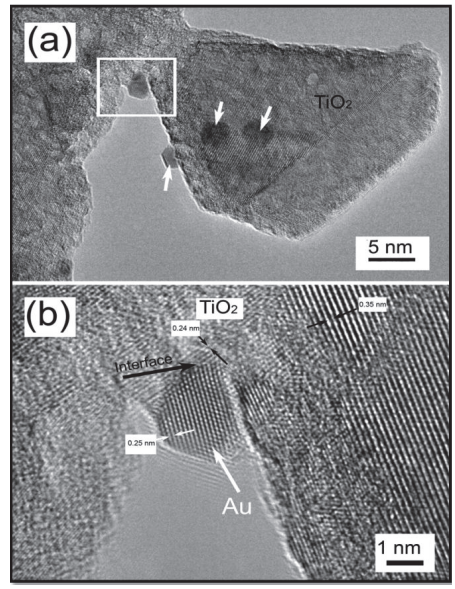

Fig. 4. HR-TEM images of modified catalyst: (a) Au nanoparticles (white arrow) attached with TiO_2 surface and (b) lattice resolved HR-TEM iamge of the Au nanoparticle and TiO_2 crystal-interface is very clear (black arrow).

Table 1. Textural properties and band gap energies of the Au-doped TiO_2 supported catalyst samples.

Samples	SSA (m^2/g)	PV (cm^3/g)	PD (nm)	E_g (eV)
Pristine sample	48.56	0.44	37.03	2.81
Thermal/plasma treated Au/TiO_2	46.13	0.34	30.51	2.66

of a single-crystal metal having (111) planes and having a sharp interface with the (004) crystal planes of TiO_2 anatase phase.

Specific surface area (SSA), pore volume (PV) and average pores diameter (PD) of the pristine and thermal/plasma treated catalysts are summarized in Table 1. The PV and PD were calculated from adsorption branch of the respective N_2 isotherm by applying Barrett, Joyner and Halenda (BJH) method. The N_2 adsorption–desorption isotherms for pristine sample and thermal/plasma treated are shown in Fig. 5. It can be depicted from plots that according to the IUPAC classification both adsorption/desorption isotherms are of a mixed type (I/II form). In fact this mixed form is probably resulted due to the presence of both micropores (0–2 nm) and mesopores (2–50 nm) that extend toward the macropore region (> 50 nm). Moreover, it is also apparent from Table 1 that Au nanoparticles size confinement has a notable effect on textural properties, especially on pore volume, of the prepared catalysts. The pristine sample showed relatively higher specific surface area

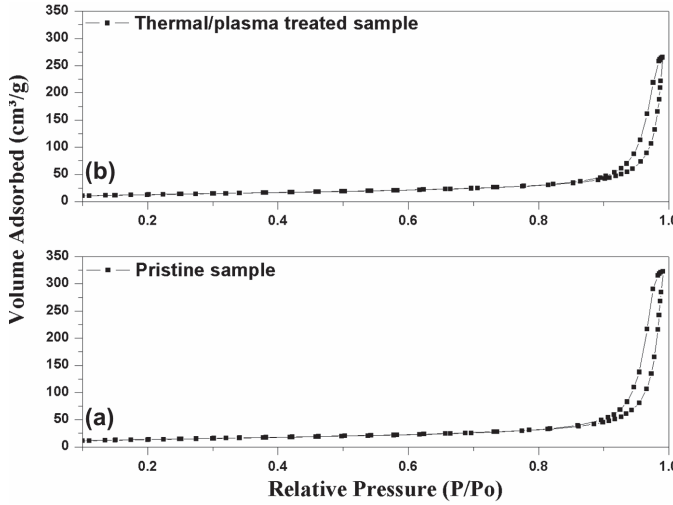

Fig. 5. N_2 adsorption–desorption isotherms for (a) pristine and (b) thermal/plasma treated sample.

and pore volume than that of thermal/plasma treated sample. For instance the BET surface and pore volume of pristine sample were 48.56 m^2/g and 0.44 cm^3/g, while for thermal/plasma treated sample both were 46.13 m^2/g and 0.34 cm^3/g, respectively which was in good agreement with the results determined by SEM.

In comparison to pristine sample, the smaller pore volume in the case of thermal/plasma treated sample is probably resulted due to partial blockage of the pores with active metal particles. Similar kinds of alterations in textural properties due to partial blockage of pores with active metal particles were also reported by various researchers in the literature.[23]

3.2. *Photocatalytic performance*

The effect of thermal/plasma modification on the photocatalytic activity was assessed by estimating the band gap and the photo-absorption spectra technique. The energy band gap (E_g) of pristine and thermal/plasma treated samples can be calculated using Eq. (1).[9]

$$\alpha h\nu = A(h\nu - E_g)^{n/2}\,, \tag{1}$$

where α, ν, E_g and A are absorption coefficient, light frequency, band gap energy and a constant, respectively, and n based on the nature of optical transition of a semiconductor for example $n = 1$ stands for direct transition whereas $n = 4$ stands for indirect transition. For TiO_2, $n = 1/2$, which corresponds to an indirect transition. The calculated band gap energy of pristine sample and thermal/plasma treated Au/TiO_2 have decreased to 2.81 eV and 2.66 ev, respectively (as shown in Table 1) in comparison to pure TiO_2 (P25) which is around 3.0–3.2 eV.[24] The

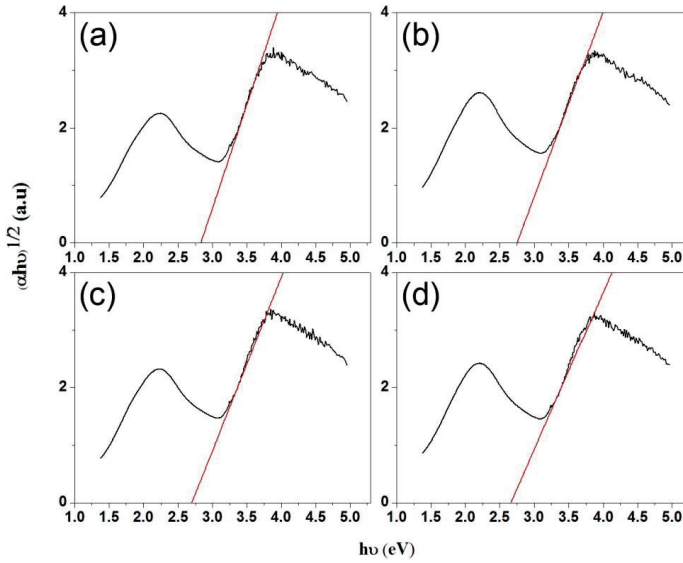

Fig. 6. (Color online) $(\alpha h\nu)^{1/2}$ versus photon energy $(h\nu)$ of Au-doped TiO_2 catalysts for (a) pristine, (b) thermal, (c) plasma and (d) thermal/plasma treated samples.

surface modification with Au particles can cause a redshift of around 0.4 eV. The decrease in band gap energy of Au-doped TiO_2 nanocomposites may be due to the band shrinkage effect which is resulted from the Au nanoparticles deposition on TiO_2 surface.[25] Figure 6 shows a plot between $(\alpha h\nu)^{1/2}$ and $h\nu$.

The sharp tangents were drawn to examine the band gaps of the fabricated catalyst and obtained reduced band gaps 2.81, 2.75, 2.69 and 2.66 eV for the pristine, thermal, plasma and combined thermal/plasma treated samples, respectively.

Figure 7 shows the photo-absorption spectra of the degraded dye solutions with respect to light-exposure durations ranging from 0–495 min. It is clearly evident that the absorption of MB gradually decreased with increasing irradiation time; however, different values of the degree of reduction were observed for each catalyst. The least degradation of around 57% was observed after illuminating the solution for 495 min under UV-Vis light that can be seen in Fig. 7(a). After incorporating the thermal/plasma modified Au-doped TiO_2 catalyst in the same sample, the MB showed a promising degradation of about 88% even after 360 min exposure to UV-Vis light, as displayed in Fig. 7(d). It can be seen that the maximum absorbance at 665 nm rapidly decreases with the increase in irradiation time and disappears almost completely after a certain time. The lack of any new-appearing peak in the course of the reaction showed that degradation had been successfully completed. These results confirm the enhanced photocatalytic activity of the modified samples in the UV light compared to untreated samples. Such enhanced photocatalytic performance can be attributed to the excellent electronic conductivity and enhanced mass transportation, which facilitates photo-induced electron transport to the

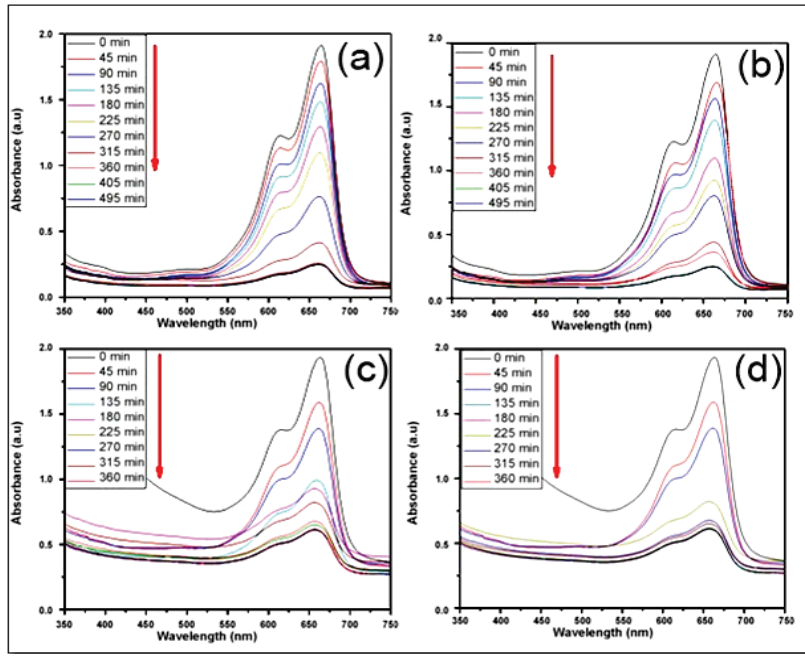

Fig. 7. (Color online) Time-dependent UV-Vis absorption spectra of (a) pristine, (b) thermally treated Au-doped TiO_2, (c) plasma treated Au-doped TiO_2 and (d) thermal/plasma treated TiO_2.

surface of the catalysts, thereby inhibiting recombination of photo-induced electrons and holes.[26]

Though the same amounts of Au nanoparticles were introduced during the catalysts synthesis, our TEM analysis showed significant changes in the diameters and population of Au nanoparticles after thermal followed by plasma treatments. Since the Au nanoparticles expedite the transport of photo-generated electrons and facilitates the longer charge separation by trapping them which in result displayed positive effect on the MB degradation.[20]

Plasma sputtering improved the uniform distribution of the catalytic active species in the catalyst by converting the large Au nanoparticles into relatively smaller nanoparticles and our results are well agreed with the reported cases.[20,27] Thus, it can be postulated that the size confinement of Au nanoparticles due to thermal/plasma process increase the number of photo-generated electrons and holes in order to contribute in the photocatalytic reaction which in result enhanced the photocatalytic activity.[27]

Furthermore, our results also showed an interesting sequence related to the photocatalytic activity of the catalyst samples. The order for MB degradation of Au-doped TiO_2 catalysts was related to type of processing done on the catalysts and the results showed MB degradation for thermal/plasma > plasma > thermal treatments > pristine samples (see Fig. 8). This sequence degradation exactly

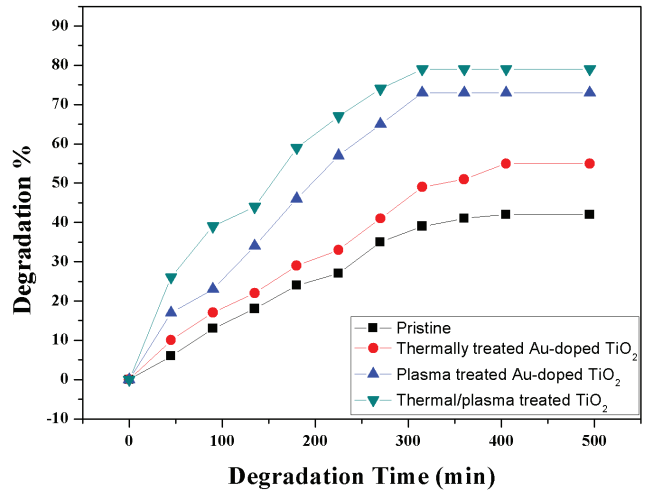

Fig. 8. (Color online) Time versus MB degradation (%) in the UV-Vis irradiation.

follows the order of band gaps obtained for all samples. The decreased band gap by the thermal/plasma treatment of Au-doped TiO_2 catalyst demonstrates the effectiveness of the synthesis catalysts for MB degradation in the UV-Vis irradiation. Based upon these results, it may be elucidated the thermal/plasma treatment controlled the morphology and population of the Au nanoparticles. The size confinement of the Au nanoparticles decreased the band gap and the increased in numbers of active sites, thus improved the quality of the Au-doped TiO_2 catalyst, which was confirmed experimentally by assessing the degradation of MB in the presence of modified catalyst.

4. Conclusion

The effect of thermal/plasma treatment on the photocatalytic performance of the Au-doped TiO_2 catalysts prepared by conventional deposition precipitation method was studied. The photocatalytic activity was gauged by assessing the degradation of MB in the presence of catalysis under UV light spectra. Our results showed that the quality of Au-doped TiO_2 catalyst was significantly improved by the thermal/plasma treatments. After the thermal/plasma treatment, the specific surface area of the Au/TiO_2 samples decreased. The thermal/plasma treatments reduced the size and increased the population of the Au nanoparticles, improved the Au/TiO_2 interface, altered the textural properties and functionally, reduced the band gaps, and these traits contributed in improving the efficiency of the modified catalysts. Obtained 88% degradation of the MB in the presence of modified catalytic compared to 57% degradation in case of unmodified catalyst, confirmed the enhanced photocatalytic performance of the modified catalyst. Concisely, combined thermal/plasma treatment is an effective method to obtain Au-doped TiO_2 with

better photocatalytic performance and modified Au-doped TiO_2 catalysts may have potential applications in waste water disinfection, energy harvesting, solar technology, air purification and many others.

Acknowledgments

The authors extend their appreciation to the Deanship of Scientific Research at King Saud University for funding the work through the research group Project No. RGP-VPP-311.

References

1. R. Leary and A. Westwood, *Carbon* **49** (2011) 741.
2. J. Zhang, Z. Xiong and X. S. Zhao, *J. Mater. Chem.* **21** (2011) 3634.
3. J. Du, X. Lai, N. Yang, J. Zhai, D. Kisailus, F. Su, D. Wang and L. Jiang, *ACS Nano* **5** (2011) 590.
4. L. M. Pastrana-Martinez, J. L. Faria, J. M. Dona-Rodriguez, C. Fernandez-Rodriguez and A. M. T. Silva, *Appl. Catal. B: Environ.* **113–114** (2012) 221.
5. G. C. Silva, R. Juarez, T. Marino, R. Molinari and H. Garcia, *J. Am. Chem. Soc.* **133** (2011) 595.
6. L. Qi, J. Yu and M. Jaroniec, *Phys. Chem. Chem. Phys.* **13** (2011) 8915.
7. N. E. Ntainjua, J. K. Edwards, A. F. Carley, J. A. Lopez-Sanchez, J. A. Moulijn, A. A. Herzing, C. J. Kiely and G. J. Hutchings, *Green Chem.* **10** (2008) 1162.
8. R. Liu, Y. Yu, K. Yoshida, G. Li, H. Jiang, M. Zhang, F. Zhao, S. Fujita and M. Arai, *J. Catal.* **269** (2010) 191.
9. C. Liu, H. Lin, S. Gao, P. Yin, L. Guo, B. Huang and Y. Dai, *Bull. Korean Chem. Soc.* **35** (2014) 441.
10. M. Haruta, N. Yamada, T. Kobayashi and S. Iijima, *J. Catal.* **115** (1989) 301.
11. K. Connelly, A. K. Wahab and H. Idriss, *Mater. Renew. Sustain. Energy* **1** (2012) 3.
12. G. C. Bond and D. T. Thompson, *Catal. Rev.* **41** (1999) 319.
13. R. Zanella, S. Giorgio, C. H. Shin, C. R. Henry and C. Louis, *J. Catal.* **222** (2004) 357.
14. M. Haruta, *Catal. Today* **36** (1997) 153.
15. J. D. Grunwaldt and A. Baiker, *J. Catal.* **181** (1999) 223.
16. S. Linic, P. Christopher and D. Ingram, *Nat. Mater.* **10** (2011) 911.
17. Z. W. Seh, S. Liu, M. Low, S. Y. Zhang, Z. Liu, A. Mlayah and M. Y. Han, *Adv. Mater.* **24** (2012) 2310.
18. A. Primo, A. Corma and H. Garcia, *Phys. Chem. Chem. Phys.* **13** (2010) 886.
19. C. Wang, B. Q. Xu, X. Wang and J. Zhao, *J. Solid State Chem.* **178** (2005) 3500.
20. A. Mahmood and S. I. Woo, *Kor. J. Chem. Eng.* **30** (2013) 1876.
21. M. A. Debeila, N. J. Coville, M. S. Scurrell and G. R. Hearne, *Appl. Catal. A: Gen.* **291** (2005) 98.
22. J. Wang, C. Liu, Y. Zhang, X. Zhu and F. He, *Catal. Today* **89** (2004) 183.
23. J. Taghavimo-Ghaddam, G. P. Knowles and A. L. Chaffee, *J. Mol. Catal. A: Chem.* **377** (2013) 115.
24. A. F. Shojaei and M. H. Loghmani, *Bull. Korean Chem. Soc.* **33** (2012) 3981.
25. M. M. Khan, S. A. Ansari, J. Lee and M. H. Cho, *J. Ind. Eng. Chem.* **19** (2013) 1845.
26. Y. H. Kim and H. C. Choi, *Bull. Korean Chem. Soc.* **34** (2013) 3586.
27. B. Z. Tian, C. Z. Li, F. Gu and H. B. Jiang, *Catal. Commun.* **10** (2009) 925.